

# Design and comparison of permanent magnetic gear and REBCO superconductor magnetic gear

EunSeok Yang<sup>a</sup>, Jonghoon Yoon<sup>b</sup>, JuKyung Cha<sup>b</sup>, Jaheum Koo<sup>b</sup>, Seungyong Hahn<sup>\*,b</sup>, and Sangjin Lee<sup>b</sup>

<sup>a</sup> Department of Future Automotive Mobility, Seoul National University, Seoul, 08826, Republic of Korea

<sup>b</sup> Department of Electrical and Computer Engineering, Seoul National University, Seoul, 08826, Republic of Korea

(Received 6 December 2024; revised or reviewed 24 December 2024; accepted 25 December 2024)

## Abstract

As environmental concerns become a global issue, wind turbines are gaining attention as a sustainable energy solution. Traditional wind turbines use a mechanical gearbox to transfer energy from the low-speed, high-torque blades to the high-speed, low-torque generator. However, mechanical gearboxes present various challenges due to mechanical contact. To address these issues, considerable research has been conducted on magnetic gears. Since magnetic gears operate without mechanical contact, they offer advantages such as high transmission efficiency and inherent overload protection. Various topologies exist for magnetic gears, and with the introduction of modulating gear topology, torque density has been significantly improved. Many studies are focused on further enhancing torque density, one of which involves the use of superconductors. This paper presents the design of a magnetic gear using REBCO superconducting coil magnets to enhance torque density compared to conventional permanent magnet magnetic gears. The design optimization was conducted using the Non-Dominated Sorting Genetic Algorithm II (NSGA-II). The performance was evaluated in terms of torque ripple, torque density, and efficiency. In the magnetic gear applying superconductor, it demonstrates performance with lower torque ripple (0.16%/0.25%), lower losses (229 kW), higher efficiency (96.35%), and higher torque density (1.086 MNm/m<sup>3</sup>).

*Keywords:* magnetic gear, permanent magnet, superconducting coil(REBCO), wind turbine

## 1. INTRODUCTION

Efforts to reduce carbon emissions are being pursued globally, and one prominent approach among these efforts is the use of renewable energy sources. In particular, wind turbines have garnered significant attention. Wind turbines transmit energy from the low-speed, high-torque blades to the high-speed, low-torque generator. In this case, energy can be transmitted through either a direct generator or a gearbox. However, due to the nature of mechanical contact, mechanical gears encounter a variety of issues, including noise, vibration, mechanical wear, and the need for lubrication, which reduce overall efficiency [1-3]. Additionally, the variable load characteristics of wind turbines make it challenging to provide adequate overload protection, which can lead to unexpected maintenance.

To address the limitations of mechanical gears, extensive research has been conducted on magnetic gears, which operate without mechanical contact and therefore mitigate the drawbacks associated with traditional mechanical gears [1, 4]. Magnetic gears offer physical separation between input and output within the gear itself [5], enabling high transmission efficiency [6] and inherent overload protection, resulting in high reliability [4].

Various topologies have been explored for magnetic gears, initially focusing on configurations that mimic traditional mechanical gears, such as worm, bevel, rack-

and-pinion, planetary, and spur gears [1, 4]. However, these early topologies demonstrated insufficient torque density, limiting their potential as substitutes for mechanical gears. The development of the coaxial modulating gear topology marked a breakthrough in increasing torque density [1], making it a widely studied topology in recent research.

Numerous studies have been dedicated to further enhancing the torque density of magnetic gears. Research has explored magnetic gears featuring Halbach arrays, spoke-type configurations [6], and asymmetric modulators [7]. Additionally, incorporating superconductors into magnetic gears has shown promise for increasing torque density. Leveraging the Meissner effect of superconductors, magnetic flux modulation effects can be maximized, and replacing permanent magnets with magnetized superconductor bulks has been investigated as a method to increase torque density.

This paper presents the design of a 6 MW coaxial modulating magnetic gear for wind turbines, utilizing REBCO superconducting coil magnets in place of permanent magnets. Section 2 discusses the design of both the permanent magnet and superconducting magnetic gears. Section 3 covers the loss calculations, while Section 4 presents a performance comparison between the two magnetic gears, examining aspects such as torque ripple, loss, torque density, and efficiency. The paper concludes with Section 5.

\* Corresponding author: hahnsy@snu.ac.kr

## 2. MAGNETIC GEAR DESIGN

### 2.1. Permanent Magnet Magnetic Gear (PMMG)

Among the various topologies of magnetic gears, this study selects the coaxial modulating gear topology. In this configuration, the fixed part determines the direction and interaction of the magnetic fields, which influences the gear ratio. When the modulator is fixed, it ensures stable modulation of the magnetic flux between the rotors. Fixing the inner or outer rotor changes the relative motion between the parts, altering the distribution of magnetic flux and, consequently, the torque and speed characteristics [2]. In this study, the outermost magnet is fixed, while the modulator and the innermost magnet rotate. If the pole pairs of the magnets are denoted as  $N_1$  and  $N_2$ , the number of pole pieces in the modulator becomes  $N_1+N_2$ . Based on the fixed part, the number of pole pieces in the modulator and the number of pole pairs in the innermost magnet determine the gear ratio, speed ratio, and torque ratio.

Modulator : Innermost Magnet

$$\text{Gear Ratio} \quad N_1+N_2 : N_2 \quad (1)$$

$$\text{Speed Ratio} \quad N_2 : N_1+N_2 \quad (2)$$

$$\text{Torque Ratio} \quad N_1+N_2 : N_2 \quad (3)$$

The design of the magnetic gear for use in wind turbines was based on the configuration presented in a previous study that employed permanent magnets [8]; further details of the design can be seen in Fig. 1. As shown in equation (2) and Fig. 1, the modulator section serves as the slow rotor, while the inner permanent magnet and inner core sections function as the fast rotor.

To identify the maximum torque for design purposes, the angle between the two rotors and the stator was varied to locate the point of maximum torque, which was then used as the basis for the design. As shown in Fig. 2, the angle between the stator and the slow rotor is defined as  $\theta_s$ , and the angle between the stator and the fast rotor is defined as  $\theta_f$ .

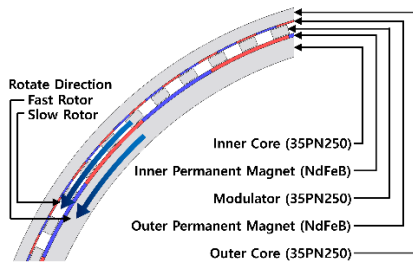


Fig. 1. Geometry of PMMG with part names, material properties, and rotation direction.

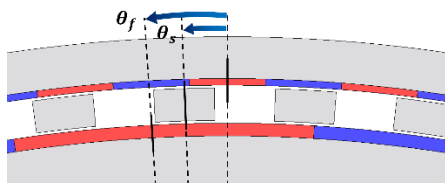


Fig. 2. Definition of  $\theta_s$  (angle between the stator and modulator) and  $\theta_f$  (angle between the stator and inner magnet).

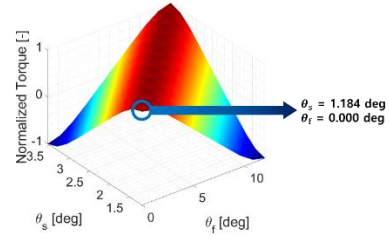


Fig. 3. Average torque as a function of  $\theta_s$  and  $\theta_f$ .

TABLE I  
SPECIFICATION OF PMMG IN SIMULATION.

Parameter	Value
Outer Pole Pairs	61
Pole Pieces	76
Inner Pole Pairs	15
Gear Ratio	76 : 15
Inner Radius	2450 mm
Inner Core Thickness	122 mm
Inner Magnet Thickness	23 mm
Inner Airgap	5 mm
Pole Pieces Fill Factor	0.5
Outer Airgap	5 mm
Outer Magnet Thickness	12 mm
Outer Core Thickness	75 mm
Outer Radius	2750 mm
Stack Length	2315.95 mm
Permenet magnet remanence magnetic field	1.2 T
Slow rotor rotating speed	12.5 rpm
Fast rotor rotating speed	63.3 rpm
Power	6 MW

The normalized average torque as a function of  $\theta_s$  and  $\theta_f$  is shown in Fig. 3. The angles that yield the maximum torque,  $\theta_s = 1.184 \text{ deg}$  and  $\theta_f = 0.000 \text{ deg}$ , were set as the design parameters to achieve maximum torque. The specifications of the PMMG (Permanent Magnet Magnetic Gear) used for the final comparison are shown in Table I [8].

### 2.2. Superconductor Magnetic Gear (SCMG)

#### 2.2.1. Initial Model for Optimization

The SCMG was optimized using Non-Dominated Sorting Genetic Algorithm II (NSGA-II) to consider multiple objective functions, with the initial model for optimization set as follows. To eliminate the need for a slip ring, the SCMG replaces only the permanent magnet in the non-rotating stator part with a superconducting coil, while maintaining the same configuration as the PMMG.

To utilize the advantage of high stability against quench in NI coil [9], an NI coil was adopted, with a double pancake (DP) racetrack design, consisting of two single pancakes (SP), chosen for the coil shape. The operating

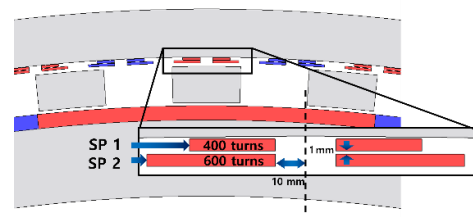


Fig. 4. Superconductor coil cross section.

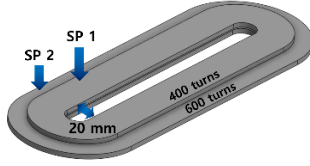


Fig. 5. Superconductor coil geometry.

TABLE II

SPECIFICATION OF INITIAL SUPERCONDUCTING COIL FOR OPTIMIZATION.

Parameter	Value
Operating temperature	30 K
Tape thickness	70 $\mu$ m
Tape width	4 mm
Inner radius	10 mm
Thickness of SP-SP Spacer	1 mm
Truns of coil 1	400
Turns of coil 2	600

temperature of the superconducting coil was set at 30 K, allowing for a temperature margin based on the boiling point of liquid hydrogen. The specifications of the coil are shown in Fig. 4, Fig. 5, and Table II. Fig. 5 represents a detailed view of the stack length direction for illustrative purposes.

### 2.2.2 NSGA-II Optimization

For optimization using NSGA-II, four input variables, three constraints, and two objective functions were defined. The equations for the constraints and the objective function are shown in Table III, followed by a detailed description of each parameter.

The first input and the second input were set as parameters to determine the overall size of the magnetic gear, with the radial ratio (RO\_ratio) and the axial length (Stack Length). The third input is the operating current  $I_{op}$  of the REBCO coil, and the fourth is the thickness of the outer core, which provides magnetic shielding. Refer to Fig. 6 for a visual representation.

The first constraint is based on magnetic shielding standards for electrical devices, set at  $< 0.5$  mT (5 gauss) at a radius of 1 m from the outer yoke [10]. The second

TABLE III

CONSTRAINTS AND OBJECTIVE FUNCTIONS OF NSGA-II OPTIMIZATION.

Constraints
Magnetic flux density at radius of 1m from the outer yoke $< 0.5$ mT
Critical current margin $> 30\%$
Power capacity = 6 MW
Objective function
f1: Maximize (Average torque / Weight of gear)
f2: Minimize (Total usage of HTS wire)

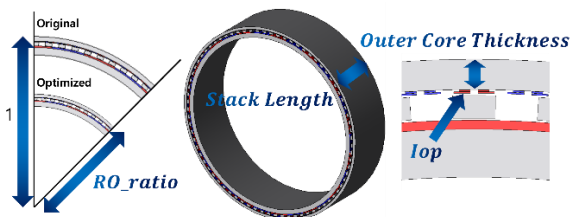
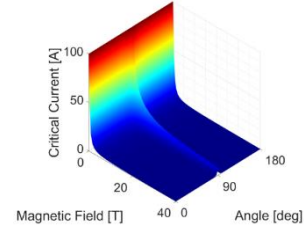
Fig. 6. Four optimization parameters: RO-ratio, Stack Length, Outer Core Thickness, and  $I_{op}$ .

Fig. 7. Critical current of REBCO tape as a function of magnetic field and angle at 30 K.

TABLE IV  
OPTIMAL RESULT OF NSGA-II OPTIMIZATION.

Parameter	PMMG	SCMG Initial Model	SCMG Optimized Model
RO_ratio	1	1	0.9993
Stack Length	2.32 m	2.32 m	0.91 m
Outer Core Thickness	75 mm	75 mm	113 mm
$I_{op}$	-	20 A	87 A
$I_c$ margin	-	14%	32%
Torque density	0.47 MNm/m <sup>3</sup>	0.47 MNm/m <sup>3</sup>	1.09 MNm/m <sup>3</sup>
Total HTS tape usage	-	577 km	235 km

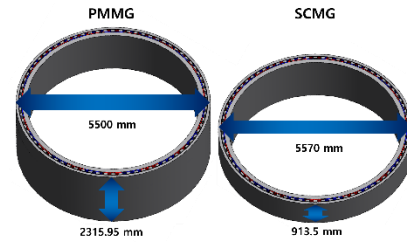


Fig. 8. Stack length and outer radius comparison between PMMG and SCMG.

constraint addresses the critical current margin of the superconducting coil. REBCO tape is sensitive not only to the magnitude of the external magnetic field but also to its angle. At 30 K, the critical current of the conductor used in this design, based on data from SuNAM, is shown in Fig. 7. Based on this data, the critical current was calculated, and a constraint was set to maintain a margin of at least 30% below the critical current. The third constraint ensures that the SCMG achieves the same power capacity as the PMMG, set at 6 MW, as the power capacity varies with the input parameters.

In magnetic gears, torque density is a critical parameter, so maximizing torque density was set as the first objective function. Additionally, because the cost is expected to be significantly influenced by the price of superconducting tape, minimizing the total amount of superconducting tape used was set as the second objective function.

The NSGA-II optimization was run with a population size of 30 and 100 generations. The final parameters for the designed SCMG are shown in Table IV. As the  $I_{op}$  of the SCMG increased, it was observed that the required volume and total tape usage to achieve the same power output decreased. The final volumes are shown in Fig. 8.

## 3. LOSS CALCULATION

### 3.1. Loss in Magnetic Gear

TABLE V  
LOSS COMPONENTS OF PMMG AND SCMG.

Parameter		Value
PMMG	PM eddy current loss	279.4 kW
	Iron eddy current loss	0.7 kW
	Iron hysteresis loss	6.1 kW
	PM eddy current loss	216.9 kW
SCMG	Iron eddy current loss	0.7 kW
	Iron hysteresis loss	11.1 kW

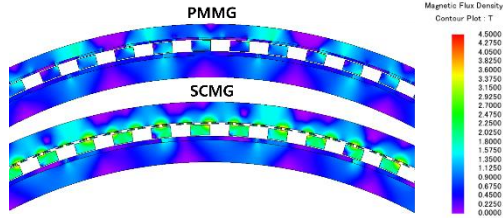


Fig. 9. Magnetic field distribution of PMMG and SCMG.

Unlike mechanical gears, magnetic gears transfer power through magnetic fields, resulting in losses within the magnetic materials. Losses in magnetic gears include eddy current loss in the permanent magnets, eddy current and hysteresis losses in the ferromagnetic cores, and bearing friction loss. In this study, bearing friction loss is not considered from the loss calculations.

With the stack length of the SCMG reduced by more than 50%, losses were expected to decrease proportionally. However, as shown in Fig. 9, the higher magnetic field of the SCMG led to greater losses than anticipated. As a result, the SCMG achieves only a 20.1% reduction in losses compared to the PMMG.

### 3.2. Loss of PMMG and SCMG

The total loss for the PMMG is 286 kW, while the SCMG has a total loss of 229 kW. For specific values of each type of loss, refer to Table V.

## 4. PERFORMANCE COMPARISON

### 4.1. Torque Ripple & Torque Density

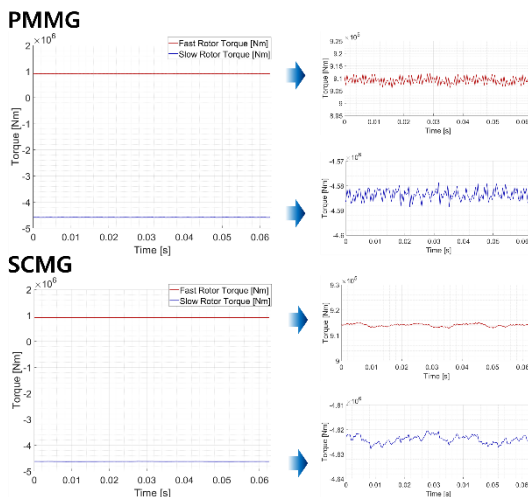


Fig. 10. Torque graph of PMMG and SCMG.

TABLE VI  
PERFORMANCE COMPARISON BETWEEN PMMG AND SCMG.

Parameter	Value	
	PMMG	SCMG
Torque ripple	0.22% / 0.67%	0.16% / 0.25%
Total loss	286 kW	229 kW
Efficiency	95.4%	96.4%
Torque density	0.465 MNm/m <sup>3</sup>	1.086 MNm/m <sup>3</sup>

Torque ripple is a primary factor that causes vibration and noise in magnetic gears. The torque waveforms are shown in Fig. 10. For the PMMG, the torque ripple is 0.22% on the slow rotor and 0.67% on the fast rotor. For the SCMG, the torque ripple is 0.16% on the slow rotor and 0.25% on the fast rotor. Compared to the SCMG, which uses an air core, the PMMG exhibits 36% higher torque ripple on the slow rotor and 165% higher on the fast rotor.

Torque density, a key metric for performance comparison, holds significant importance in magnetic gears, which are essential for power transmission in wind turbines. The torque density is 0.465 MNm/m<sup>3</sup> for the PMMG and 1.086 MNm/m<sup>3</sup> for the SCMG, showing that the SCMG has a 133% higher torque density compared to the PMMG.

### 4.2. Efficiency

The equation for calculating efficiency is given by (4) [1]. The losses were determined based on the calculations in Section 3.

$$\text{Efficiency} = \frac{\text{Output power}}{\text{Input power}} = \frac{\text{Output power}}{\text{Total loss} + \text{Output power}} \quad (4)$$

The efficiency of the PMMG is 95.44%, while the SCMG has an efficiency of 96.35%, indicating that the SCMG exhibits 0.91% higher efficiency than the PMMG.

### 4.3. Performance Comparison

Table VI summarizes the performance comparison results of the two magnetic gears.

## 5. CONCLUSION

In this paper, a 6 MW-class magnetic gear was designed using superconductors and optimized with NSGA-II. A performance comparison was conducted between this design and a conventional magnetic gear that uses permanent magnets. The result highlights the advantage of superconductors in achieving the same power output as permanent magnets with smaller volume.

SCMG exhibits lower torque ripple at 0.16%/0.25% compared to PMMG's 0.22%/0.67%. It also shows reduced total loss (229 kW) and higher efficiency (96.35%) than PMMG (286 kW/95.44%). Additionally, SCMG outperforms PMMG in torque density, achieving 1.086 MNm/m<sup>3</sup> over 0.465 MNm/m<sup>3</sup>.

One of the limitations of this study is the omission of AC loss in superconductors, which results from variations in external magnetic fields. Future research should address this by incorporating AC loss into the analysis, along with examining the effects of heat generation on performance degradation.

## ACKNOWLEDGMENT

This work was supported in part by National R&D Program through the National Research Foundation of Korea(NRF) funded by Ministry of Science and ICT(2022M3I9A1073924), and in part by the Applied Superconductivity Center, Electric Power Research Institute of Seoul National University.

## REFERENCES

- [1] Ruiz-Ponce Gerardo, et al., "A review of magnetic gear technologies used in mechanical power transmission," *Energies*, vol. 4, no. 16, pp. 1721, 2023.
- [2] N. W. Frank and H. A. Toliyat, "Gearing ratios of a magnetic gear for wind turbines," *2009 IEEE International Electric Machines and Drives Conference*, pp. 1224-1230, 2009.
- [3] K. Atallah and D. Howe, "A novel high-performance magnetic gear," *IEEE Transactions on Magnetics*, vol. 37, no. 4, pp. 2844-2846, 2001.
- [4] P. M. Tlali, R. -J. Wang, and S. Gerber, "Magnetic gear technologies: A review," *2014 International Conference on Electrical Machines (ICEM)*, Berlin, Germany, pp. 544-550, 2014
- [5] McGilton Ben, et al., "Review of magnetic gear technologies and their applications in marine energy," *IET Renewable Power Generation*, vol. 12, no. 2, pp. 174-181, 2018.
- [6] P. O. Rasmussen, T. O. Andersen, F. T. Jorgensen, and O. Nielsen, "Development of a high-performance magnetic gear," *IEEE Transactions on Industry Applications*, vol. 41, no. 3, pp. 764-770, 2005.
- [7] B. Dai, K. Nakamura, Y. Suzuki, Y. Tachiya, and K. Kuritani, "Cogging Torque Reduction of Integer Gear Ratio Axial-Flux Magnetic Gear for Wind-Power Generation Application by Using Two New Types of Pole Pieces," *IEEE Transactions on Magnetics*, vol. 58, no. 8, pp. 1-5, 2022.
- [8] M. Desvaux, et al., "Magnetic losses and thermal analysis in a magnetic gear for wind turbine," *2018 Thirteenth International Conference on Ecological Vehicles and Renewable Energies (EVER)*, pp. 1-7, 2018.
- [9] S. Hahn, et al., "Current status of and challenges for no-insulation HTS winding technique," *低温工学*, vol. 53, no. 1, pp. 2-9, 2018.
- [10] International Commission on Non-Ionizing Radiation Protection. "Guidelines on limits of exposure to static magnetic fields," *Health Physics*, vol. 96, no. 4, pp. 504-514, 2009.